

Toward digital twins for ocular applications: mathematical modeling, simulation and order reduction

Thomas Saigre¹, Christophe Prud'homme¹, Marcela Szopos²

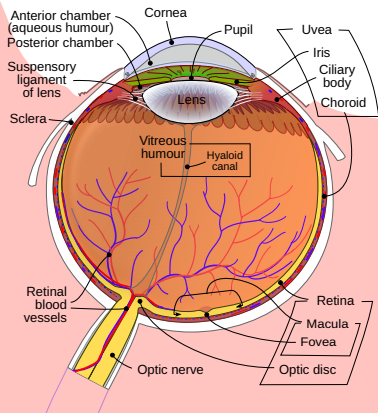
¹Institut de Recherche Mathématique Avancée, UMR 7501 Université de Strasbourg et CNRS

²Université Paris Cité, CNRS, MAP5, F-75006 Paris, France

Colloquium CASA Eindhoven
18th June 2025



Motivation: understand ocular **physiology** and **pathology**



Rhcastilhos, from Wikipedia

- ▶ The **eye** is a complex organ, with a **multilayered structure**, numerous multiscale and multiphysics phenomena involved.
- ▶ **Measurements:** complex to perform on human subjects^a, scarce data, mostly available on surface^b.
- 💡 Present work: focus on **heat transfer** and **aqueous humor flow dynamics**.

^aRosenbluth & Fatt. *Exp. Eye Res.* (1977)

^bPurslow & Wolffsohn. *Eye Contact Lens.* (2005)

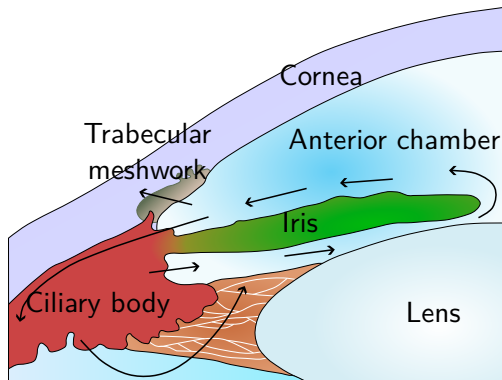
Motivation: understand ocular **physiology** and **pathology**

- ▶ The **anterior chamber** (AC) is filled with **aqueous humor** (AH), whose dynamics is crucial for the ocular health^a,
- ▶ understand the **AH flow dynamics** and **heat transfer** is important for **drug distribution**^b, and **therapeutic interventions** (laser treatment, corneal cell sedimentation^c, etc.).

^aDvoriashyna *et al.* *Ocular Fluid Dynamics*. (2019)

^bBhandari. *J Control Release*. (2021)

^cKinoshita *et al.* *N Engl J Med*. (2018)



Adapted from Ramakrishnan *et al.*

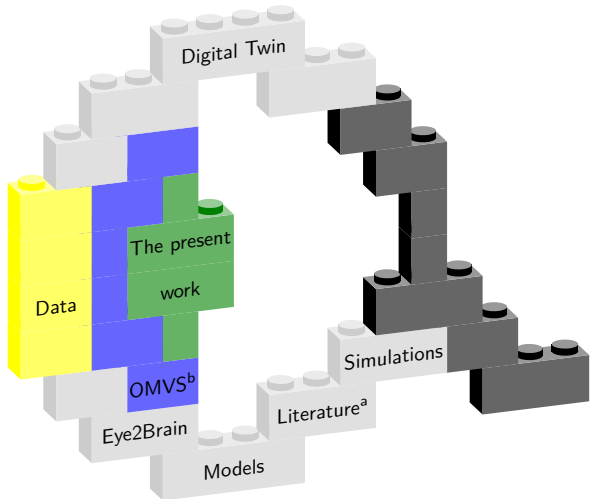
Figure 1: Production and drainage of AH in the eye.

Aim: build a digital twin of the eye

- ▶ State-of-the-art: **digital models^a** of the eye.
- ▶ Toward a **digital shadow**: data from **previous studies** and **measurements** to validate and enhance the models.
- ▶ Final goal: a **digital twin** = virtual replica of the eye, in real-time connection with the physical entity.

^aScott (1988), Ng et al. (2007), Dvoriashyna et al. (2019)...

^bSala et al. *Int J Numer Methods Biomed Eng.* (2023)



Methodology

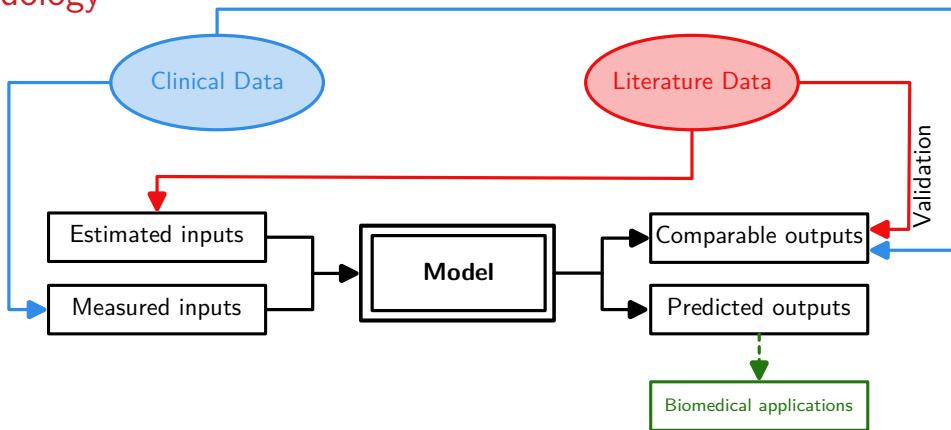
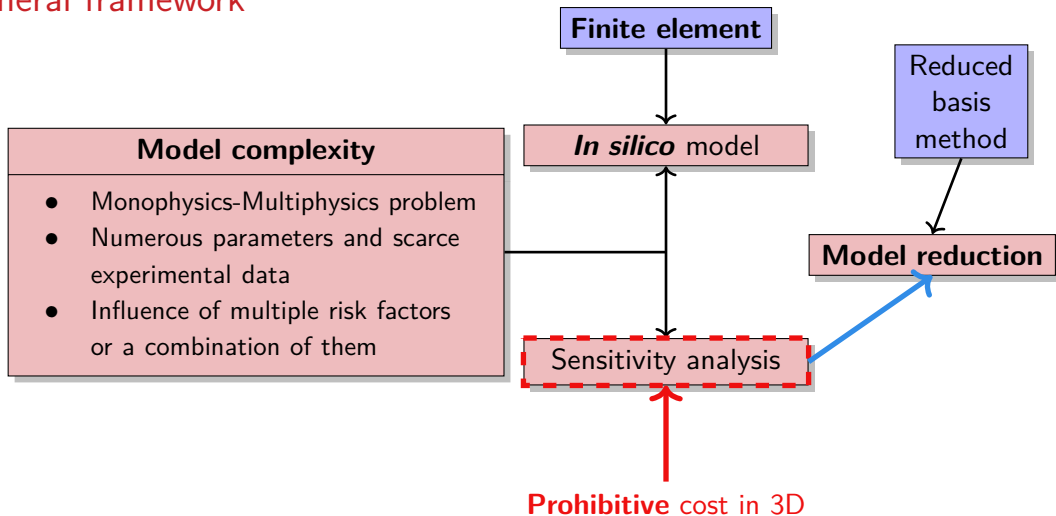


Figure 2: Methodology for the development of patient-specific models, adapted from^a.

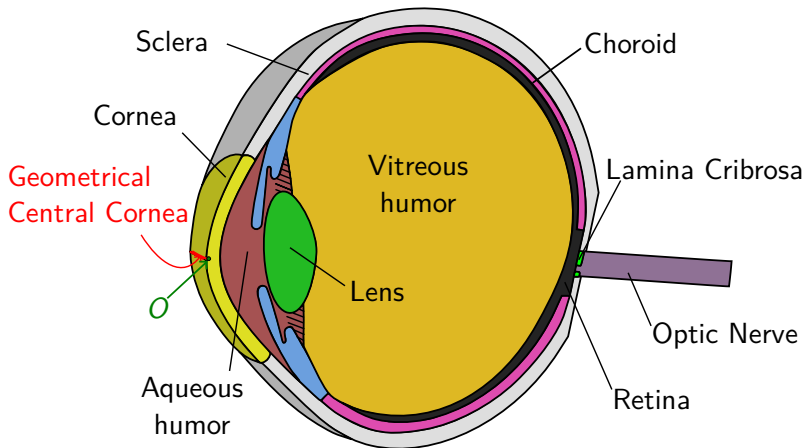
^aSala *et al.* *International Journal for Numerical Methods in Biomedical Engineering*. (2023)

General framework



Mathematical modeling of heat transfer and aqueous humor flow mechanisms in the eye

Geometrical model^a



^aSala *et al.* The ocular mathematical virtual simulator: A validated multiscale model for hemodynamics and biomechanics in the human eye. *Int J Numer Method Biomed Eng.* (2023)

Biophysical model^{ab}

- ▶ Incompressible fluid, constant density,
- ▶ The steady flow of the aqueous humor is governed by the Navier–Stokes equations:

Navier-Stokes equations

$$\rho(\mathbf{u} \cdot \nabla) \mathbf{u} - \nabla \cdot (2\mu \underline{\underline{D}}(\mathbf{u}) - p \underline{\underline{I}}) =$$

Boussinesq approximation

$$-\rho\beta(T - T_{\text{ref}})\mathbf{g}$$

in Ω_{AH} ,

Incompressibility

$$\nabla \cdot \mathbf{u} = 0$$

in Ω_{AH} ,

Heat transfer equation

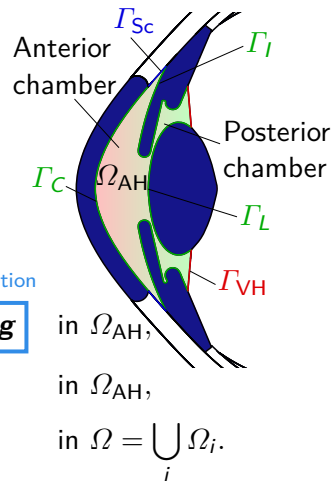
$$\rho C_p \mathbf{u} \cdot \nabla T - k_i \nabla^2 T = 0$$

in $\Omega = \bigcup_i \Omega_i$.

+ Boundary and Interface conditions.

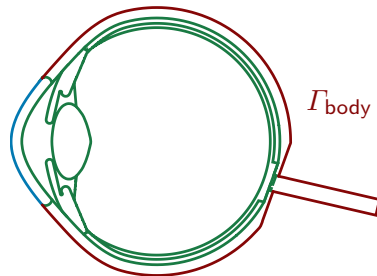
^aScott. *Physics in Medicine and Biology*. (1988), Ng & Ooi. *Comput Methods Programs Biomed*. (2006), Li et al. *Int J Numer Method Biomed Eng*. (2010)...

^bWang et al. *BioMedical Engineering OnLine*. (2016), Dvoriashyna et al. *Mathematical Models of Aqueous Production, Flow and Drainage*. (2019)...



Biophysical Model: Boundary Conditions

- ▶ Interface conditions:
$$\begin{cases} T_i = T_j, \\ k_i(\nabla T_i \cdot \mathbf{n}_i) = -k_j(\nabla T_j \cdot \mathbf{n}_j) \end{cases}$$
 over $\partial\Omega_i \cap \partial\Omega_j$.
- ▶ Robin condition on Γ_{body} : $-k_i \frac{\partial T}{\partial \mathbf{n}} = h_{\text{bl}}(T - T_{\text{bl}}).$ Γ_{amb}
- ▶ Neumann condition on Γ_{amb} :
$$-k_i \frac{\partial T}{\partial \mathbf{n}} = h_{\text{amb}}(T - T_{\text{amb}}) + \sigma \varepsilon (T^4 - T_{\text{amb}}^4) + E.$$
- ▶ Conditions on velocity: $\mathbf{u} = \mathbf{0}$ on $\Gamma_C \cup \Gamma_I \cup \Gamma_L \cup \Gamma_{\text{VH}} \cup \Gamma_{\text{Sc}}.$



^aScott. *Physics in Medicine and Biology*. (1988)

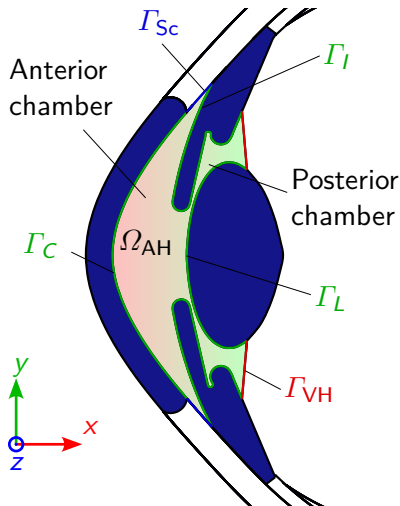
Biophysical Model: Boundary Conditions

- ▶ Interface conditions: $\begin{cases} T_i = T_j, \\ k_i(\nabla T_i \cdot \mathbf{n}_i) = -k_j(\nabla T_j \cdot \mathbf{n}_j) \end{cases}$
over $\partial\Omega_i \cap \partial\Omega_j$.

- ▶ Robin condition on Γ_{body} : $-k_i \frac{\partial T}{\partial \mathbf{n}} = h_{\text{bl}}(T - T_{\text{bl}})$.

- ▶ Linearized Neumann condition^a on Γ_{amb} :
 $-k_i \frac{\partial T_i}{\partial \mathbf{n}} = h_{\text{amb}}(T - T_{\text{amb}}) + h_r(T - T_{\text{amb}}) + E,$
with $h_r = 6 \text{ W m}^{-2} \text{ K}^{-1}$.

- ▶ Conditions on velocity:
 $\mathbf{u} = \mathbf{0}$ on $\Gamma_C \cup \Gamma_I \cup \Gamma_L \cup \Gamma_{\text{VH}} \cup \Gamma_{\text{Sc}}$.



^aScott. *Physics in Medicine and Biology*. (1988)

Parameter dependent model

Symbol	Name	Dimension	Baseline value	Range
T_{amb}	Ambient temperature	[K]	298	[283.15, 303.15]
T_{bl}	Blood temperature	[K]	310	[308.3, 312]
h_{amb}	Ambient air convection coefficient	$[W\ m^{-2}\ K^{-1}]$	10 ^a	[8, 100]
h_{bl}	Blood convection coefficient	$[W\ m^{-2}\ K^{-1}]$	65 ^b	[50, 110]
h_r	Radiation heat transfer coefficient	$[W\ m^{-2}\ K^{-1}]$	6 ^c	–
E	Evaporation rate	$[W\ m^{-2}]$	40 ^c	[20, 320]
k_{lens}	Lens conductivity	$[W\ m^{-1}\ K^{-1}]$	0.4 ^b	[0.21, 0.544]
k_{cornea}	Cornea conductivity	$[W\ m^{-1}\ K^{-1}]$	0.58 ^d	–
$k_{sclera} = k_{iris} =$	Eye envelope	$[W\ m^{-1}\ K^{-1}]$	1.0042 ^e	–
$k_{lamina} = k_{opticNerve}$	components conductivity			
$k_{aqueousHumor}$	Aqueous humor conductivity	$[W\ m^{-1}\ K^{-1}]$	0.28 ^d	–
$k_{vitreousHumor}$	Vitreous humor conductivity	$[W\ m^{-1}\ K^{-1}]$	0.603 ^c	–
$k_{choroid} = k_{retina}$	Vascular beds conductivity	$[W\ m^{-1}\ K^{-1}]$	0.52 ^f	–
ε	Emissivity of the cornea	[–]	0.975 ^a	–

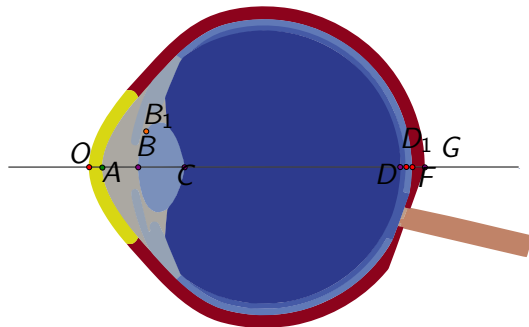
^a Mapstone (1968), ^b J J W Lagendijk (1982), ^c Scott (1988), ^d Emery et al. (1975), ^e Ng et al. (2007), ^f IT'IS Foundation (2024).

Parameters and output of interest

- ▶ Geometrical parameters may play a role^a, but not considered in this work.
- ▶ **A parameter:** we set
 $\mu = (T_{\text{amb}}, T_{\text{bl}}, h_{\text{amb}}, h_{\text{bl}}, E, k_{\text{lens}})$
 in $D^\mu \subset \mathbb{R}^6$.
- ▶ $\bar{\mu} \in D^\mu$ is the **baseline value** of the parameters.

^aBhandari. *J Control Release*. (2021)

- ▶ Locations of interest based on literature^{bcd}:

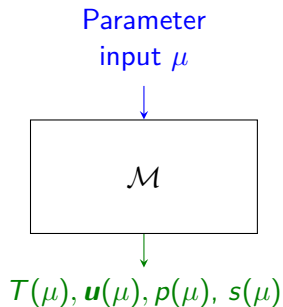


^bScott. *Physics in Medicine and Biology*. (1988)

^cNg & Ooi. *Comput. Biol. Med.* (2007)

^dLi et al. *Int J Numer Method Biomed Eng.* (2010)

Summary



Model $\mathcal{M}_{\text{HF}}(\mu)$

- ▶ **Heat transfer** in the whole eye,
- ▶ coupled with AH **fluid dynamics** in the AC and the PC.

Model $\mathcal{M}_{\text{H}}(\mu)$

- ▶ Simplified version of $\mathcal{M}_{\text{HF}}(\mu)$.
- ▶ **Heat transfer** in the whole eye, with
- ▶ linearized radiative conditions.

Full order computational framework

Discrete geometry

- ▶ Performed with Salome meshing library, using NETGEN^a meshing algorithm.
- ▶ The full pipeline to generate the mesh is available on GitHub^b.

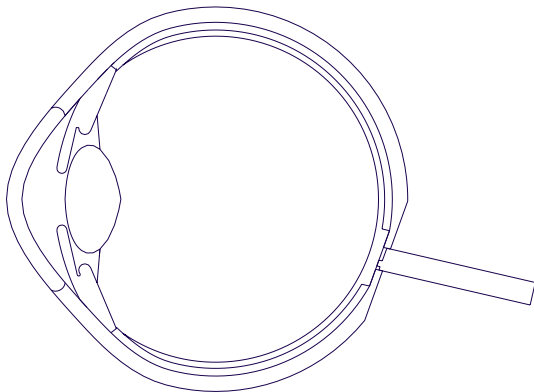


Figure 3: Geometry of the eye.

^aJ. Schöberl. *Computing and Visualization in Science*. (1997)

^bV. Chabannes, C. Prud'homme, T. Saigre, et al. *A 3D geometrical model and meshing procedures for the human eyeball*. (2024) github.com/feelpp/mesh.eye

Discrete geometry

- ▶ Performed with Salome meshing library, using NETGEN^a meshing algorithm.
- ▶ The full pipeline to generate the mesh is available on GitHub^b.
- ▶ The mesh generated by Salome is quite coarse.

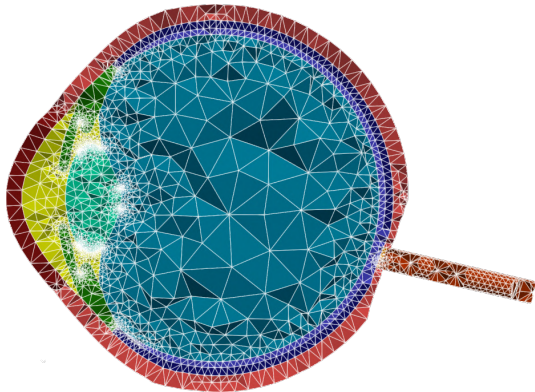


Figure 3: Original mesh M, $4.64 \cdot 10^5$ tetrahedrons.

^aJ. Schöberl. *Computing and Visualization in Science*. (1997)

^bV. Chabannes, C. Prud'homme, T. Saigre, et al. *A 3D geometrical model and meshing procedures for the human eyeball*. (2024) github.com/feelpp/mesh.eye

Discrete geometry

- ▶ Performed with Salome meshing library, using NETGEN^a meshing algorithm.
- ▶ The full pipeline to generate the mesh is available on GitHub^b.
- ▶ The mesh generated by Salome is quite coarse.
- ▶ We refine the mesh around the AC and PC.
- ▶ For the verification step, we generate a family of meshes of various refinement.

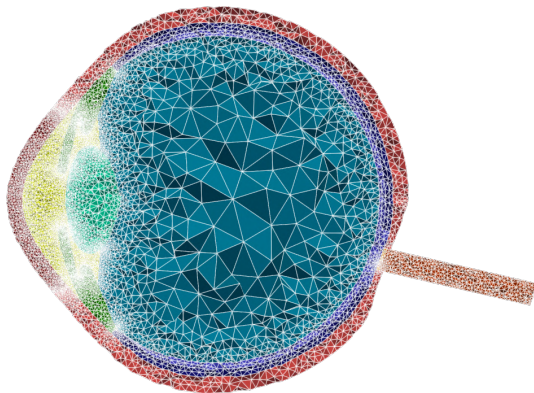


Figure 3: Mesh refined around AC and PC Mr, $9.4 \cdot 10^5$ elements.

^aJ. Schöberl. *Computing and Visualization in Science*. (1997)

^bV. Chabannes, C. Prud'homme, T. Saigre, et al. *A 3D geometrical model and meshing procedures for the human eyeball*. (2024) github.com/feelpp/mesh.eye

Mesh adaptation and refinement

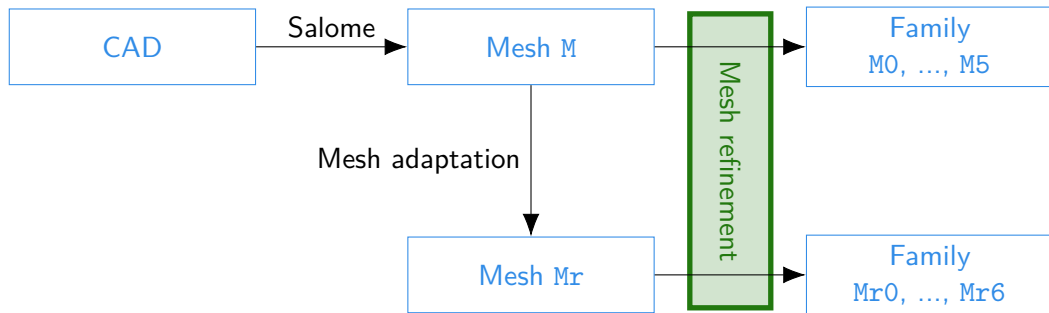


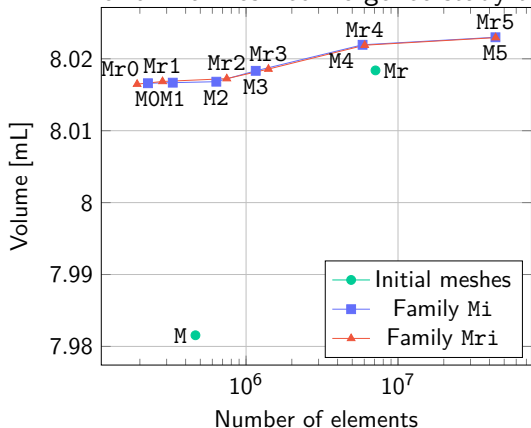
Figure 4: Pipeline to generate the geometry and mesh families.

- All the meshes are available in an open-source repository^a.

^aT. Saigre *et al.* *Mesh and configuration files to perform coupled heat+fluid simulations on a realistic human eyeball geometry with Feel++*. (2024)

Verification steps: preservation of the volume

- Solve a Laplacian problem with manufactured solution and compare convergence with the FEM theory.
- Perform a mesh convergence study to ensure the mesh is well refined.



- The volume tends toward a constant value, around 8.02 mL.
- The geometric model overestimates this value, but still remains in an acceptable physiological range^a.

^aHeymsfield *et al.* *Anatomy & Physiology*. (2016)

Continuous and discrete problem \mathcal{M}_H

We set $V := H^1(\Omega)$.

Problem considered

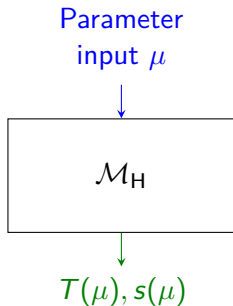
Given $\mu \in D^\mu$, evaluate the output of interest

$$s(\mu) = \ell(T(\mu); \mu),$$

where $T(\mu) \in V$ is the solution of

$$a(T(\mu), v; \mu) = f(v; \mu) \quad \forall v \in V.$$

The bilinear form $a(\cdot, \cdot; \mu)$ and the linear form $f(\cdot; \mu)$ are defined by the variational formulation of the problem.



Continuous and discrete problem \mathcal{M}_H

$$a(T, v; \mu) = f(v; \mu),$$

with:

$$a(T, v; \mu) := k_{\text{lens}} \int_{\Omega_{\text{lens}}} \nabla T \cdot \nabla v \, dx + \sum_{i \neq \text{lens}} k_i \int_{\Omega_i} \nabla T \cdot \nabla v \, dx +$$

$$\int_{\Gamma_{\text{amb}}} [h_{\text{amb}} T + h_r T] v \, d\sigma + \int_{\Gamma_{\text{body}}} h_{\text{bl}} T v \, d\sigma$$

$$f(v; \mu) := \int_{\Gamma_{\text{amb}}} [h_{\text{amb}} T_{\text{amb}} + h_r T_{\text{amb}} - E] v \, d\sigma + \int_{\Gamma_{\text{body}}} h_{\text{bl}} T_{\text{bl}} v \, d\sigma.$$

The bilinear form $a(\cdot, \cdot; \mu)$ and the linear form $f(\cdot; \mu)$ are defined by the variational formulation of the problem.

Continuous and discrete problem \mathcal{M}_H

We set $V := H^1(\Omega)$. Denote by $V_h \subset V$ a finite-dimensional subspace of V of dimension \mathcal{N} .

High-fidelity model

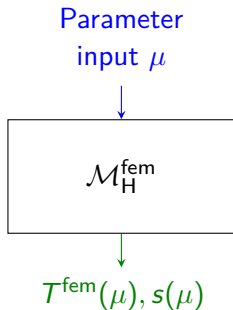
Given $\mu \in D^\mu$, evaluate the output of interest

$$s(\mu) = \ell(T^{\text{fem}}(\mu); \mu),$$

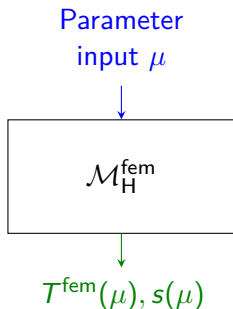
where $T^{\text{fem}}(\mu) \in V_h$ is the solution of

$$a(T^{\text{fem}}(\mu), v; \mu) = f(v; \mu) \quad \forall v \in V_h.$$

The bilinear form $a(\cdot, \cdot; \mu)$ and the linear form $f(\cdot; \mu)$ are defined by the variational formulation of the problem.



Continuous and discrete problem \mathcal{M}_H



High fidelity resolution

Input: $\mu \in D^\mu$,

- ▶ Construct $\underline{\underline{\mathbf{A}}}(\mu)$, $\mathbf{f}(\mu)$ and $\mathbf{L}_k(\mu)$,
- ▶ Solve $\underline{\underline{\mathbf{A}}}(\mu) \mathbf{T}^{\text{fem}}(\mu) = \mathbf{f}(\mu)$,
- ▶ Compute outputs $s(\mu) = \mathbf{L}_k(\mu)^T \mathbf{T}^{\text{fem}}(\mu)$.

Output: Numerical solution $\mathbf{T}^{\text{fem}}(\mu)$ and outputs $s(\mu)$.

High Fidelity model $\mathcal{M}_H^{\text{fem}}$

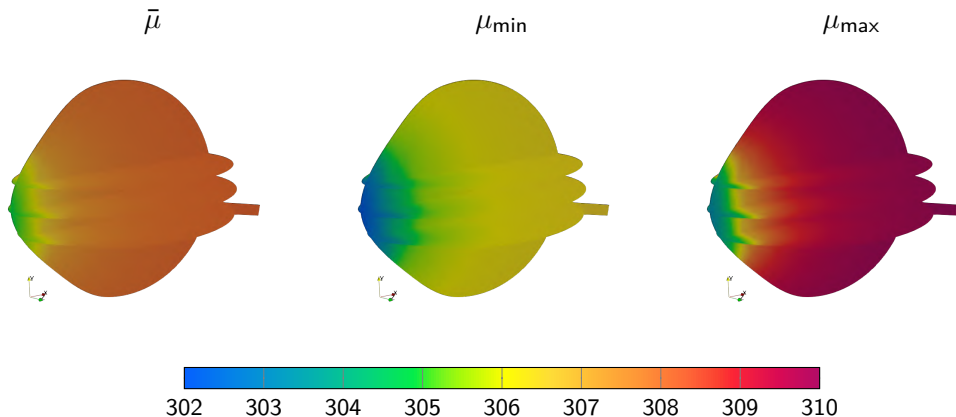
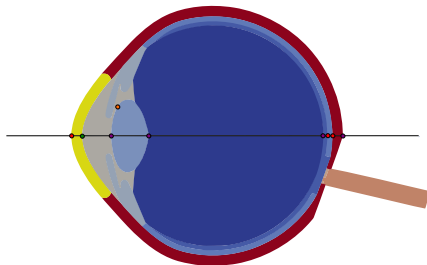
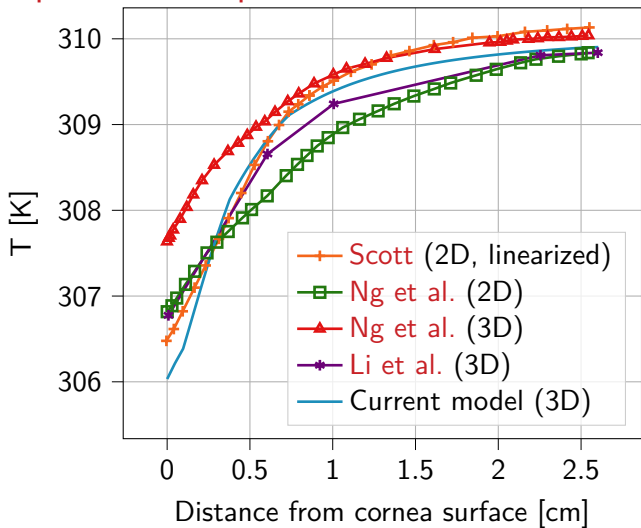
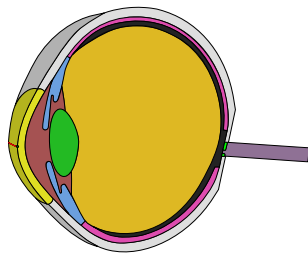
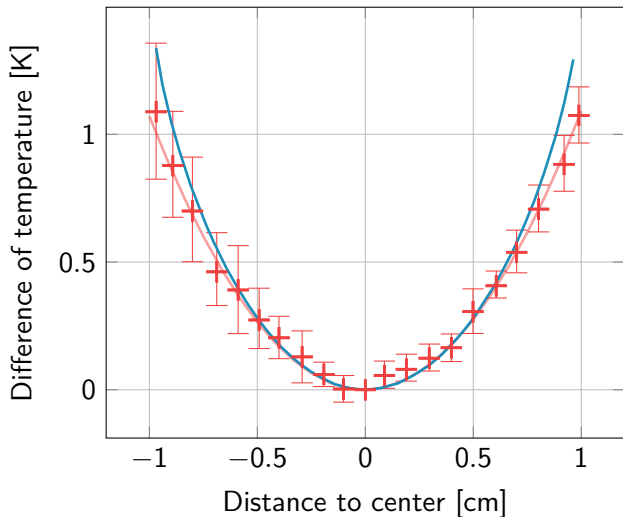


Figure 5: Distribution of the temperature [K] in the eyeball from the linear model.

Comparison with previous **numerical** studies



Validation: **measured** values over the GCC

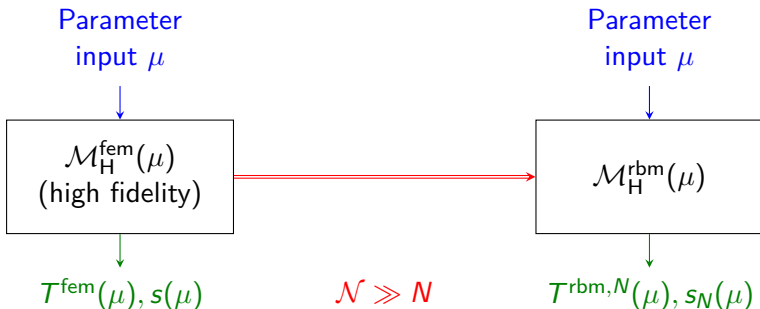


^aEfron *et al.* *Current Eye Research*. (1989)

Reduced order computational framework

Model Order Reduction

- ▶ **Goal:** replicate input-output behavior of the high fidelity model $\mathcal{M}_H^{\text{fem}}$ with a reduced order model $\mathcal{M}_H^{\text{rbm}}$,
- ▶ with a procedure stable and efficient.



Model Order Reduction

Mathematical and numerical methods for model order reduction:

- ▶ Proper orthogonal decomposition^a
- ▶ Certified Reduced Basis method^b
- ▶ Non-Intrusive Reduced Basis^c
- ▶ Machine learning techniques, such as Physics-Informed Neural Networks^d

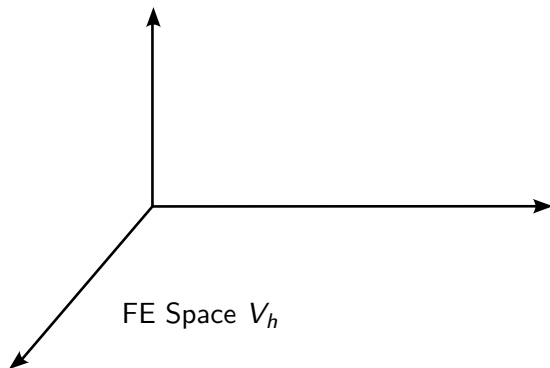
^aKerschen *et al.* *Nonlinear Dynamics*. (2005)

^bPrud'homme *et al.* *Journal of Fluids Engineering*. (2002)

^cChakir & Maday. *Comptes Rendus Mathématique*. (2009)

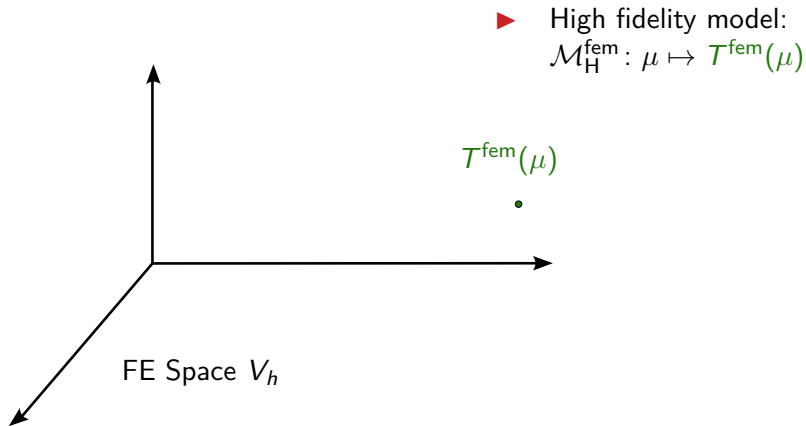
^dRaissi *et al.* *Journal of Computational Physics*. (2019)

Reduced basis method^a



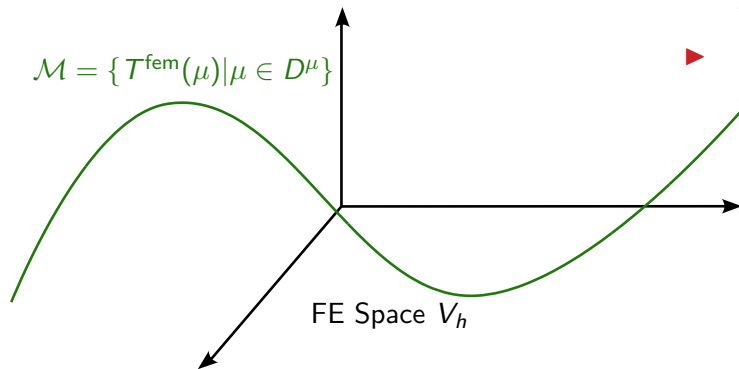
^aPrud'homme *et al.* *Journal of Fluids Engineering*. (2002)

Reduced basis method^a



^aPrud'homme *et al.* *Journal of Fluids Engineering*. (2002)

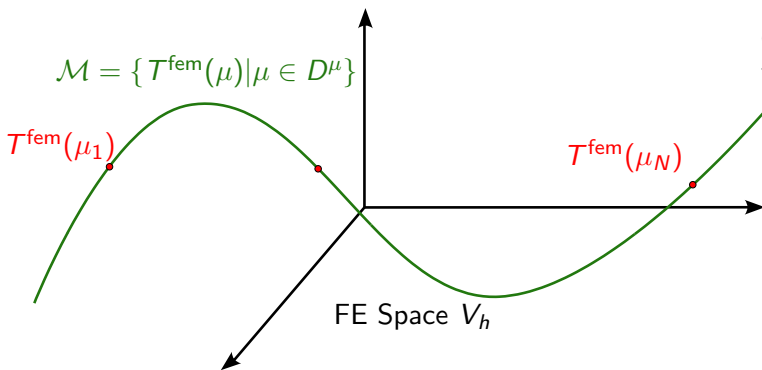
Reduced basis method^a



- ▶ High fidelity model:
 $\mathcal{M}_H^{\text{fem}}: \mu \mapsto T^{\text{fem}}(\mu)$
- ▶ Manifold of solutions:
 $\mathcal{M} = \{T^{\text{fem}}(\mu), \mu \in D^\mu\}$

^aPrud'homme *et al.* *Journal of Fluids Engineering*. (2002)

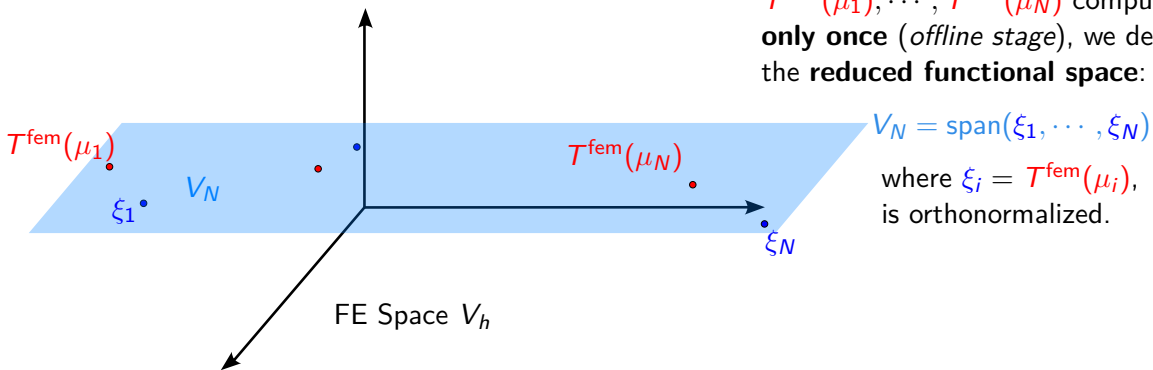
Reduced basis method^a



- From a set of **snapshots** $T^{\text{fem}}(\mu_1), \dots, T^{\text{fem}}(\mu_N)$ computed **only once** (*offline stage*), we define the **reduced functional space**:

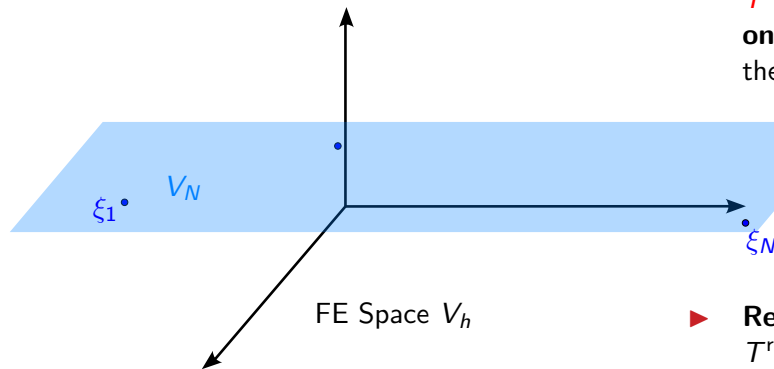
^aPrud'homme *et al.* *Journal of Fluids Engineering*. (2002)

Reduced basis method^a



^aPrud'homme *et al.* *Journal of Fluids Engineering*. (2002)

Reduced basis method^a



- From a set of **snapshots** $T^{\text{fem}}(\mu_1), \dots, T^{\text{fem}}(\mu_N)$ computed **only once** (*offline stage*), we define the **reduced functional space**:

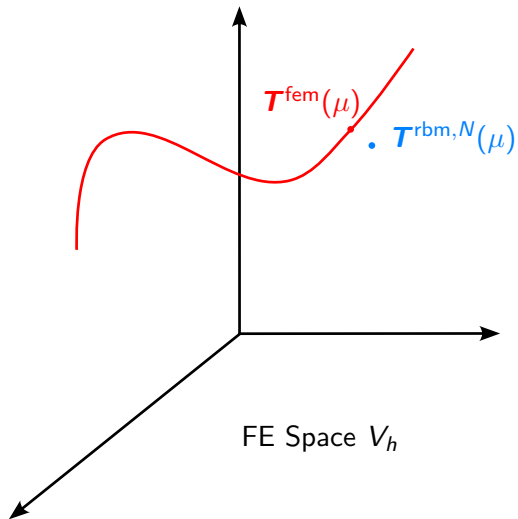
$$V_N = \text{span}(\xi_1, \dots, \xi_N)$$

where $\xi_i = T^{\text{fem}}(\mu_i)$,
is orthonormalized.

- **Reduced solution (*online stage*):**
 $T^{\text{rbm},N}(\mu)$ solution of the PDE
on V_N , **independent** of \mathcal{N} .

^aPrud'homme *et al.* *Journal of Fluids Engineering*. (2002)

Certified error bound $\Delta_N(\mu)^a$

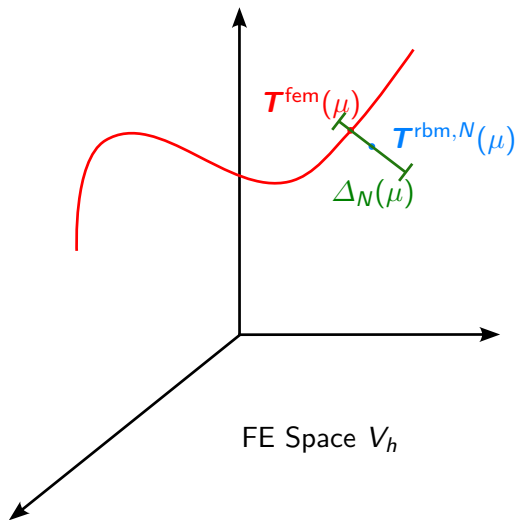


For $\mu \in D^\mu$, we define the error:

$$e(\mu) = T^{\text{fem}}(\mu) - T^{\text{rbm},N}(\mu).$$

^aPrud'homme *et al.* *Journal of Fluids Engineering*. (2002)

Certified error bound $\Delta_N(\mu)^a$



For $\mu \in D^\mu$, we define the error:

$$e(\mu) = T^{\text{fem}}(\mu) - T^{\text{rbm},N}(\mu).$$

We require this error bound to be:

- ▶ **Rigorous:** $\|e(\mu)\|_X \leq \Delta_N(\mu)$,
- ▶ **sharp:** $\frac{\Delta_N(\mu)}{\|e(\mu)\|_X} \leq \eta_{\max}(\mu)$,
- ▶ **efficient:** the computation of $\Delta_N(\mu)$ does not depend on N .

^aPrud'homme *et al.* *Journal of Fluids Engineering*. (2002)

Greedy algorithm

Algorithm 1: Greedy algorithm to construct the reduced basis.

Input: $\mu_0 \in D^\mu$, $\Xi_{\text{train}} \subset D^\mu$ and $\varepsilon_{\text{tol}} > 0$

$S \leftarrow [\mu_0];$

while $\Delta_N^{\max} > \varepsilon_{\text{tol}}$ **do**

$\mu^* \leftarrow \arg \max_{\mu \in \Xi_{\text{train}}} \Delta_N(\mu)$ (and $\Delta_N^{\max} \leftarrow \max_{\mu \in \Xi_{\text{train}}} \Delta_N(\mu)$);

$V_{N+1} \leftarrow \{\boldsymbol{\xi} = \mathbf{T}^{\text{fem}}(\mu^*)\} \cup V_N;$

Append μ^* to S ;

$N \leftarrow N + 1;$

end

Output: Sample S , reduced basis V_N

Time of execution

Implementation in the Feel++ library.

	Finite element resolution $T^{\text{fem}}(\mu)$			Reduced model $T^{\text{rbm},N}(\mu), \Delta_N(\mu)$
	\mathbb{P}_1	\mathbb{P}_2 (np=1)	\mathbb{P}_2 (np=12)	
Problem size	$\mathcal{N} = 207\,845$	$\mathcal{N} = 1\,580\,932$		$N = 10$
t_{exec}	5.534 s	62.432 s	10.76 s	2.88×10^{-4} s
speed-up	11.69	1	5.80	2.17×10^5

Table 1: Times of execution, using mesh M3 for high fidelity simulations.

Results over a sampling $\Xi_{\text{test}} \subset D^\mu$ of 100 parameters

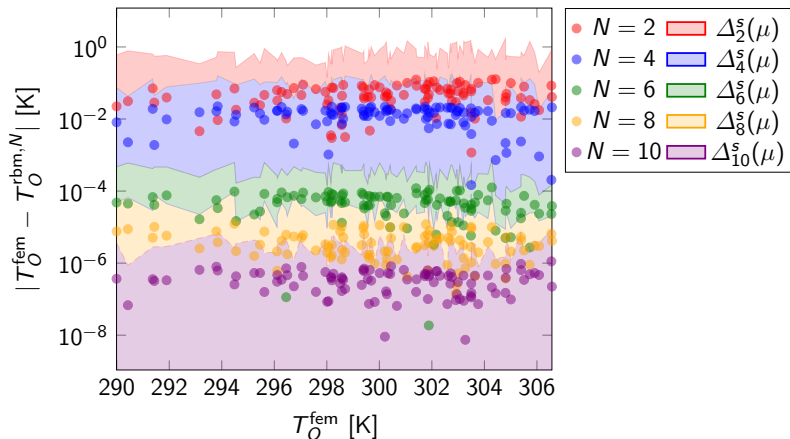


Figure 6: Error on RBM for various reduced basis sizes with error bound $\Delta_N(\mu)$.

Results over a sampling $\Xi_{\text{test}} \subset D^\mu$ of 100 parameters

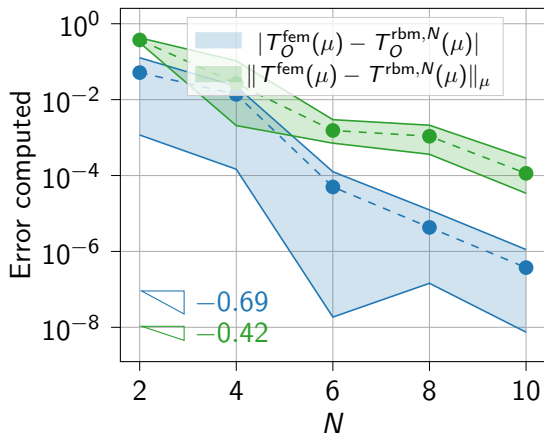


Figure 6: Convergence of the errors on the field and the output on point O .

Sensitivity analysis

Sensitivity analysis

- ▶ **Quantifies** the effect of input parameters on the output.
- ▶ Two studies were carried:
 1. **Deterministic** sensitivity analysis: all parameters are set to their baseline values, except for one, which varies within the ranges found in the literature,
 2. **Stochastic** sensitivity analysis: all parameters are considered as random variables.

Sobol' indices^a

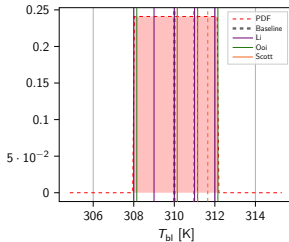
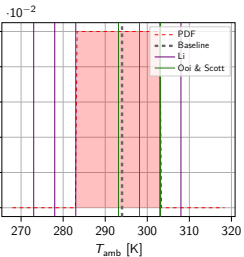
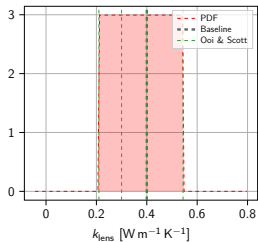
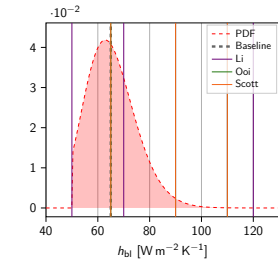
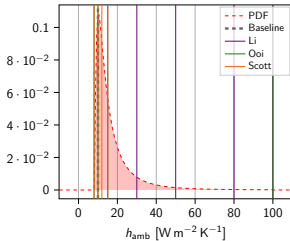
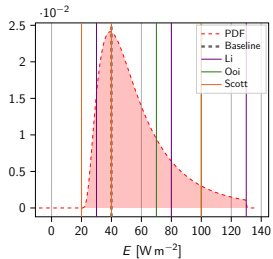
- ▶ $\mu = (\mu_1, \dots, \mu_n) \in D^\mu$,
- ▶ $\mu_i \sim X_i$ where $(X_i)_i$ is a family of **independent** random variables.
- ▶ Distributions X_i selected from data available in the literature.
- ▶ Output $s_N(\mu) \sim Y = f(X_1, \dots, X_n)$.

Sobol' indices

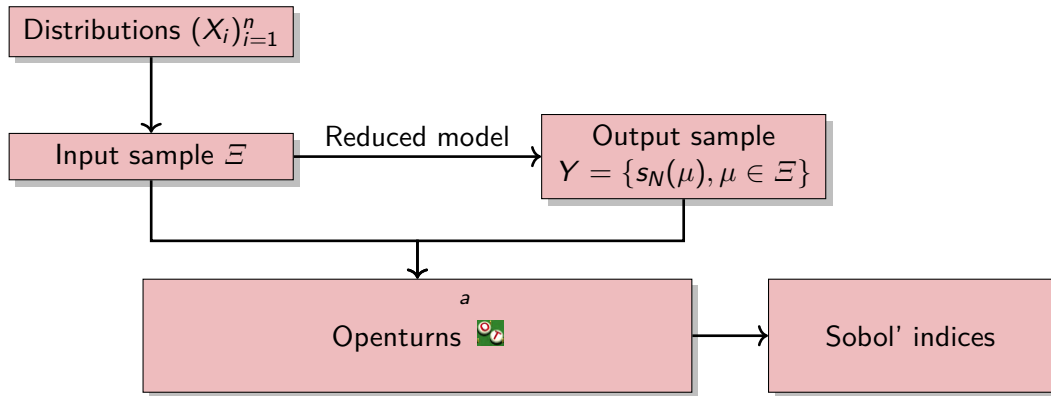
- ▶ **First-order indices:** $S_j = \frac{\text{Var}(\mathbb{E}[Y|X_j])}{\text{Var}(Y)}$ effect of one parameter on the output
- ▶ **Total-order indices:** $S_j^{\text{tot}} = \frac{\text{Var}(\mathbb{E}[Y|X_{(-j)}])}{\text{Var}(Y)}$ interaction of all parameters but one on the output
where $X_{(-j)} = (X_1, \dots, X_{j-1}, X_{j+1}, \dots, X_n)$.

^aSobol. *Sensitivity Estimates for Nonlinear Mathematical Models*. (1993)

Input parameters distributions



Stochastic sensitivity analysis



^aBaudin *et al.* *Handbook of Uncertainty Quantification*. (2016)

Stochastic sensitivity analysis

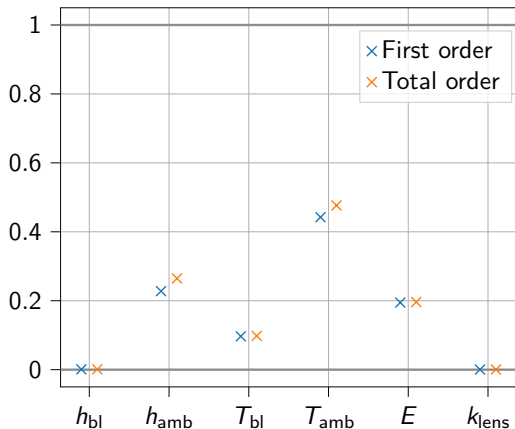
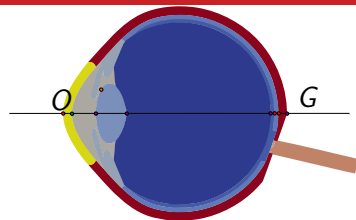


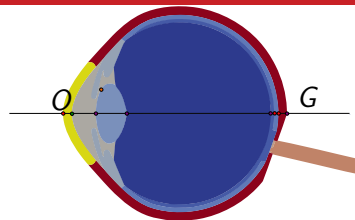
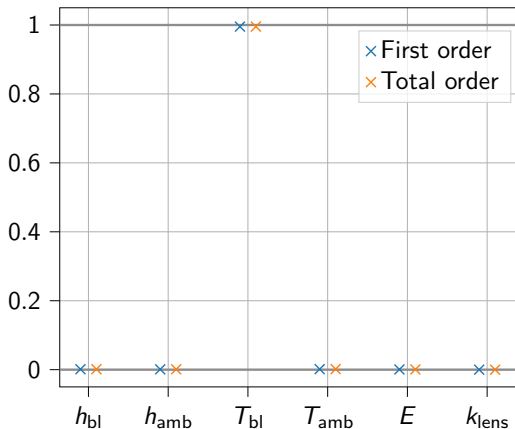
Figure 7: Sobol' indices: temperature at point O .



Temperature at the level of the **cornea**:

- ▶ **significantly** influenced by T_{amb} , h_{amb} (external factors) and E , T_{bl} (subject specific parameters) → need for measurements/better model for these contributions,
- ▶ **minimally** influenced by k_{lens} , h_{bl} → can be fixed at baseline value,
- ▶ **high order** interactions on T_{amb} , h_{amb} .

Stochastic sensitivity analysis



Temperature at the back of the eye:

- ▶ only influenced by the blood temperature.

Figure 7: Sobol' indices: temperature at point G.

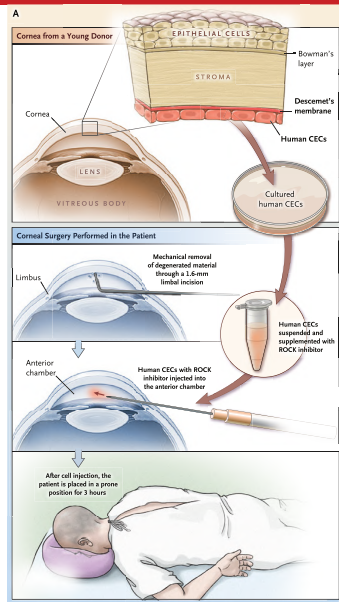
Heat transfer coupled with aqueous humor flow

Motivation: Endothelial cells sedimentation

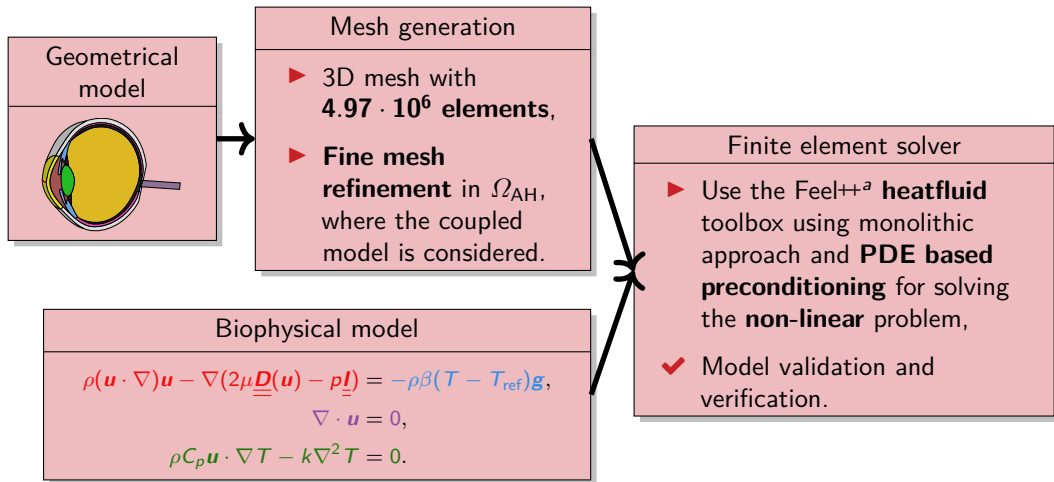
- ▶ AH flow plays a significant role in heat distribution, and intraocular pressure^a.
- ▶ Focus on the **wall shear stress** of the AH.
- ♥ Medical application: **corneal endothelial cell sedimentation** in the cornea^b.

^aDvoriashyna *et al.* *Ocular Fluid Dynamics*. (2019)

^bKinoshite *et al.* *N Engl J Med*. (2018) (Figure extracted from this reference)



Computational framework of \mathcal{M}_{HF}



^aC. Prud'homme, *et al.* Feel++ Release V111. (2024)

Pressure and velocity: impact of the posture

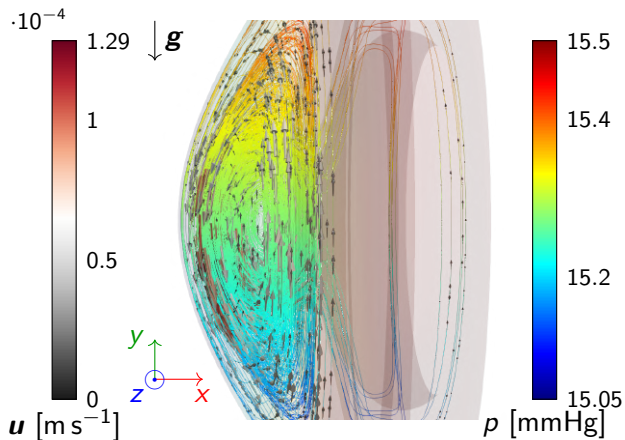


Figure 8: Standing position.

► Recirculation of the AH,

- ^aWang *et al.* BioMedical Engineering OnLine. (2016)
^bAbdelhafid *et al.* Recent Devel. in Mathematical, Statistical and Computational Sciences. (2021)
^cMurgoitio-Esandi *et al.* Translational Vision Science & Technology. (2023)

Pressure and velocity: impact of the posture

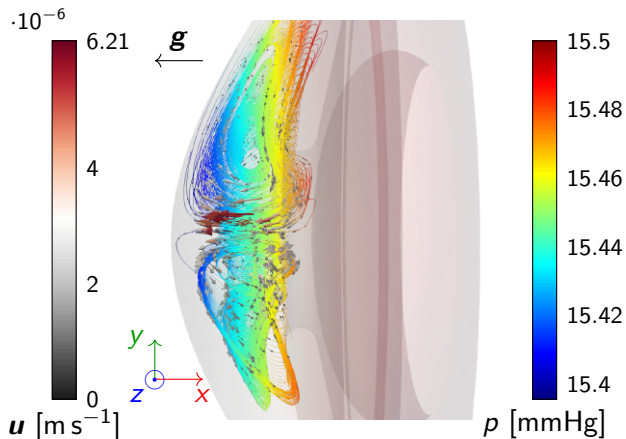


Figure 8: Prone position.

- **Recirculation** of the AH,
- Formation of a **Krukenberg's spindle**, in good agreement with clinical observations and previous studies^{abc}

^aWang *et al.* BioMedical Engineering OnLine. (2016)

^bAbdelhafid *et al.* Recent Devel. in Mathematical, Statistical and Computational Sciences. (2021)

^cMurgoitio-Esandi *et al.* Translational Vision Science & Technology. (2023)

Pressure and velocity: impact of the posture

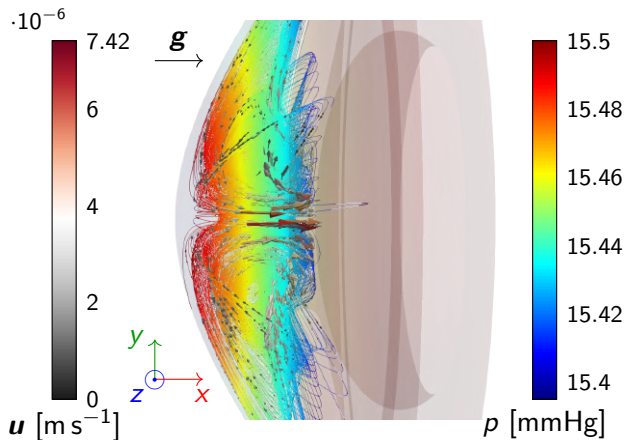


Figure 8: Supine position.

- ▶ **Recirculation** of the AH,
- ▶ Formation of a **Krukenberg's spindle**, in good agreement with clinical observations and previous studies^{abc}
- ▶ Fluid dynamics is **strongly influenced by the position of the patient**.

^aWang *et al.* BioMedical Engineering OnLine. (2016)

^bAbdelhafid *et al.* Recent Devel. in Mathematical, Statistical and Computational Sciences. (2021)

^cMurgoitio-Esandi *et al.* Translational Vision Science & Technology. (2023)

Wall shear stress

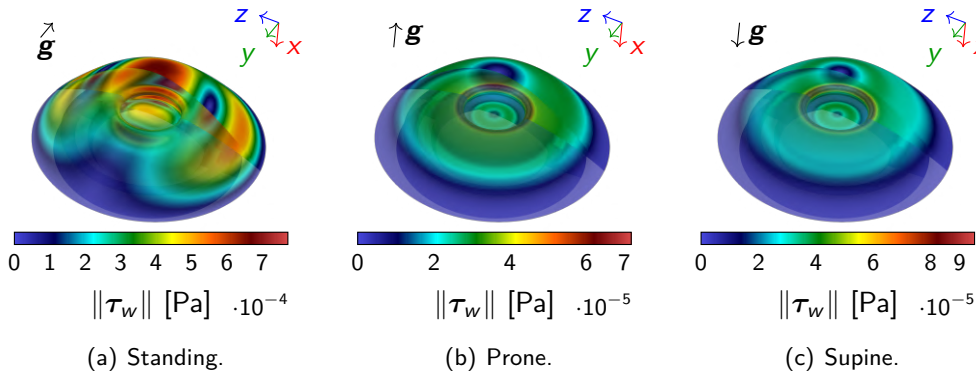


Figure 9: Wall shear stress distribution on the corneal endothelium for the three postural orientations.

Wall shear stress

- ▶ The WSS distribution is **impacted** by the postural orientation and the ambient temperature.
- ▶ **Application:** Control the temperature to enhance the diffusion and the sedimentation of the cells during the treatment.

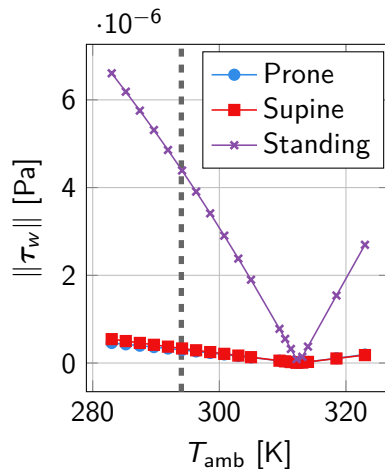


Figure 9: Mean wall shear stress on the corneal surface.

Conclusion and perspectives

- 👍 **Heat transport model in the human eye:** FEM simulations, validation against experimental data,
- 👍 **Reduced model** with a **certified error bound**,
- 👍 **Sensitivity analysis:** computation of Sobol' indices, highlight of the impact of some parameters on the outputs of interest.

📖 T. Saigre, C. Prud'homme, M. Szopos. Model order reduction and sensitivity analysis for complex heat transfer simulations inside the human eyeball. *Int J Numer Methods Biomed Eng.* (2024)

📖 T. Saigre, C. Prud'homme, M. Szopos. Associated dataset (publicly available).

DOI: 10.5281/ZENODO.13907890 *Zenodo.* (2024)

Conclusion and perspectives

- 👍 **Couple heat transfer with AH dynamics:** assess the impact of postural orientation and environmental conditions on the flow and its properties.
- 📄 T. Saigre, V. Chabannes, C. Prud'homme, M. Szopos. A coupled fluid-dynamics-heat transfer model for 3D simulations of the aqueous humor flow in the human eye. *CMBE2024 Proceedings*. (2024)
- 📄 T. Saigre, C. Prud'homme, M. Szopos, V. Chabannes. Mesh and configuration files to perform coupled heat+fluid simulations on a realistic human eyeball geometry with Feel++, DOI: 10.5281/ZENODO.13886143 *Zenodo*. (2024)
- 📄 Thomas Saigre. "Mathematical modeling, simulation and reduced order modeling of ocular flows and their interactions: Building the Eye's Digital Twin". *Theses. Université de Strasbourg*, Dec. 2024

Conclusion and perspectives

► Enhance the model:

- **Geometrical model:** take into account geometrical parameters,
- **Fluid dynamics:** modeling the production and drainage of aqueous humor to assess their impact.

👁 **Clinical perspective:** assess the corneal cell sedimentation after injection.

📄 T. Saigre, V. Chabannes, G. Guidoboni, C. Prud'homme, M. Szopos, SP. Srinivas. Effect of Cooling of the Ocular Surface on Endothelial Cell Sedimentation in Cell Injection Therapy: Insights from Computational Fluid Dynamics. (2025), to appear in IOVS.

► Steps towards a **digital twin** of the eye:

- incorporate patient-specific data,
- enhance predictive modeling and personalized medical applications.

Thank you for your attention!

Bibliography

- [Abd+21] Farah Abdelhafid et al. “Operator Splitting for the Simulation of Aqueous Humor Thermo-Fluid-Dynamics in the Anterior Chamber”. en. In: *Recent Developments in Mathematical, Statistical and Computational Sciences*. Ed. by D. Marc Kilgour et al. Vol. 343. Series Title: Springer Proceedings in Mathematics & Statistics. Cham: Springer International Publishing, 2021, pp. 489–499.
- [Bau+16] Michaël Baudin et al. “OpenTURNS: An Industrial Software for Uncertainty Quantification in Simulation”. In: *Handbook of Uncertainty Quantification*. Ed. by Roger Ghanem, David Higdon, and Houman Owhadi. Cham: Springer International Publishing, 2016, pp. 1–38.
- [BBS20] Ajay Bhandari, Ankit Bansal, and Niraj Sinha. “Effect of aging on heat transfer, fluid flow and drug transport in anterior human eye: A computational study”. en. In: *Journal of Controlled Release* 328 (Dec. 2020), pp. 286–303.
- [Bha21] Ajay Bhandari. “Ocular Fluid Mechanics and Drug Delivery: A Review of Mathematical and Computational Models”. en. In: *Pharmaceutical Research* 38.12 (Dec. 2021), pp. 2003–2033.
- [Cha+24] Vincent Chabannes et al. *A 3D geometrical model and meshing procedures for the human eyeball*. Sept. 2024.
- [Chr+24] Christophe Prud’homme et al. *feelpp/feelpp: Feel++ Release V111 preview.9*. Mar. 2024.

Bibliography

- [CM09] Rachida Chakir and Yvon Maday. “Une méthode combinée d’éléments finis à deux grilles/bases réduites pour l’approximation des solutions d’une E.D.P. paramétrique”. *fr. In: Comptes Rendus. Mathématique* 347.7-8 (2009). Publisher: Elsevier, pp. 435–440.
- [Dvo+19] Mariia Dvoriashyna et al. “Mathematical Models of Aqueous Production, Flow and Drainage”. *en. In: Ocular Fluid Dynamics*. Ed. by Giovanna Guidoboni, Alon Harris, and Riccardo Sacco. Series Title: Modeling and Simulation in Science, Engineering and Technology. Cham: Springer International Publishing, 2019, pp. 227–263.
- [Eme+75] A. F. Emery et al. “Microwave Induced Temperature Rises in Rabbit Eyes in Cataract Research”. *en. In: Journal of Heat Transfer* 97.1 (Feb. 1975), pp. 123–128.
- [EYB89] N. Efron, G. Young, and N. A. Brennan. “Ocular surface temperature”. *eng. In: Current Eye Research* 8.9 (Sept. 1989), pp. 901–906.
- [Hey+16] Steven B Heymsfield et al. “Adult Human Ocular Volume: Scaling to Body Size and Composition”. *In: Anatomy & Physiology* 6.5 (2016).
- [ITI24] IT’IS Foundation. *Thermal Conductivity*. 2024.
- [J J82] J J W Lagendijk. “A mathematical model to calculate temperature distributions in human and rabbit eyes during hyperthermic treatment”. *In: Physics in Medicine & Biology* 27.11 (Nov. 1982), pp. 1301–1311.

Bibliography

- [Ker+05] Gaetan Kerschen et al. “The Method of Proper Orthogonal Decomposition for Dynamical Characterization and Order Reduction of Mechanical Systems: An Overview”. en. In: *Nonlinear Dynamics* 41.1-3 (Aug. 2005), pp. 147–169.
- [Kin+18] Shigeru Kinoshita et al. “Injection of Cultured Cells with a ROCK Inhibitor for Bullous Keratopathy”. en. In: *New England Journal of Medicine* 378.11 (Mar. 2018), pp. 995–1003.
- [KS10] Andreas Karampatzakis and Theodoros Samaras. “Numerical model of heat transfer in the human eye with consideration of fluid dynamics of the aqueous humour”. In: *Physics in Medicine and Biology* 55.19 (Oct. 2010), pp. 5653–5665.
- [Li+10] Eric Li et al. “Modeling and simulation of bioheat transfer in the human eye using the 3D alpha finite element method (α FEM)”. In: *International Journal for Numerical Methods in Biomedical Engineering* 26.8 (2010), pp. 955–976.
- [Map68] R. Mapstone. “Measurement of corneal temperature”. en. In: *Experimental Eye Research* 7.2 (Apr. 1968), 237–IN29.
- [Mur+23] Javier Murgoitio-Esandi et al. “A Mechanistic Model of Aqueous Humor Flow to Study Effects of Angle Closure on Intraocular Pressure”. In: *Translational Vision Science & Technology* 12.1 (Jan. 2023), p. 16.

Bibliography

- [NO06] E.Y.K. Ng and E.H. Ooi. “FEM simulation of the eye structure with bioheat analysis”. en. In: *Computer Methods and Programs in Biomedicine* 82.3 (June 2006), pp. 268–276.
- [NO07] E.Y.K. Ng and E.H. Ooi. “Ocular surface temperature: A 3D FEM prediction using bioheat equation”. en. In: *Computers in Biology and Medicine* 37.6 (June 2007), pp. 829–835.
- [ON08] Ean-Hin Ooi and Eddie Yin-Kwee Ng. “Simulation of aqueous humor hydrodynamics in human eye heat transfer”. en. In: *Computers in Biology and Medicine* 38.2 (Feb. 2008), pp. 252–262.
- [Pru+02] C. Prud’homme et al. “Reliable Real-Time Solution of Parametrized Partial Differential Equations: Reduced-Basis Output Bound Methods”. en. In: *Journal of Fluids Engineering* 124.1 (Mar. 2002), pp. 70–80.
- [PW05] Christine Purslow and James S. Wolffsohn. “Ocular Surface Temperature: A Review”. en. In: *Eye & Contact Lens: Science & Clinical Practice* 31.3 (May 2005), pp. 117–123.
- [RF77] Robert F. Rosenbluth and Irving Fatt. “Temperature measurements in the eye”. en. In: *Experimental Eye Research* 25.4 (Oct. 1977), pp. 325–341.
- [RPK19] M. Raissi, P. Perdikaris, and G. E. Karniadakis. “Physics-informed neural networks: A deep learning framework for solving forward and inverse problems involving nonlinear partial differential equations”. In: *Journal of Computational Physics* 378 (2019), pp. 686–707.

Bibliography

- [RRK13] R Ramakrishnan, Shalmali Ranaut, and Mona Khurana. “Aqueous Humor Dynamics”. en. In: *Diagnosis and Management of Glaucoma*. Jaypee Brothers Medical Publishers (P) Ltd., 2013, pp. 76–76.
- [Sai+24a] Thomas Saigre et al. “A coupled fluid-dynamics-heat transfer model for 3D simulations of the aqueous humor flow in the human eye”. In: *8th International Conference on Computational and Mathematical Biomedical Engineering – CMBE2024 Proceedings*. Vol. 2. Arlington (Virginia), United States: P. Nithiarasu and R. Löhner (Eds.), June 2024, pp. 508–512.
- [Sai+24b] Thomas Saigre et al. *Mesh and configuration files to perform coupled heat+fluid simulations on a realistic human eyeball geometry with Feel++*. Oct. 2024.
- [Sai+25] Thomas Saigre et al. *Effect of Cooling of the Ocular Surface on Endothelial Cell Sedimentation in Cell Injection Therapy: Insights from Computational Fluid Dynamics*. To appear in IOVS. 2025.
- [Sai24] Thomas Saigre. “Mathematical modeling, simulation and reduced order modeling of ocular flows and their interactions: Building the Eye’s Digital Twin”. Theses. Université de Strabourg, Dec. 2024.
- [Sal+23] Lorenzo Sala et al. “The ocular mathematical virtual simulator: A validated multiscale model for hemodynamics and biomechanics in the human eye”. en. In: *International Journal for Numerical Methods in Biomedical Engineering* (Nov. 2023), e3791.

Bibliography

- [Sch97] Joachim Schöberl. “NETGEN An advancing front 2D/3D-mesh generator based on abstract rules”. In: *Computing and Visualization in Science* 1.1 (July 1997), pp. 41–52.
- [Sco88] J A Scott. “A finite element model of heat transport in the human eye”. In: *Physics in Medicine and Biology* 33.2 (Feb. 1988), pp. 227–242.
- [Sob93] Ilya M. Sobol. “Sensitivity Estimates for Nonlinear Mathematical Models”. In: 1993.
- [SPS24a] Thomas Saigre, Christophe Prud'homme, and Marcela Szopos. *Model order reduction and sensitivity analysis for complex heat transfer simulations inside the human eyeball*. Oct. 2024.
- [SPS24b] Thomas Saigre, Christophe Prud'homme, and Marcela Szopos. “Model order reduction and sensitivity analysis for complex heat transfer simulations inside the human eyeball”. en. In: *International Journal for Numerical Methods in Biomedical Engineering* 40.11 (Sept. 2024), e3864.
- [Wan+16] Wenjia Wang et al. “Fluid and structure coupling analysis of the interaction between aqueous humor and iris”. en. In: *BioMedical Engineering OnLine* 15.S2 (Dec. 2016), p. 133.

Linearization of the radiative transfer equation

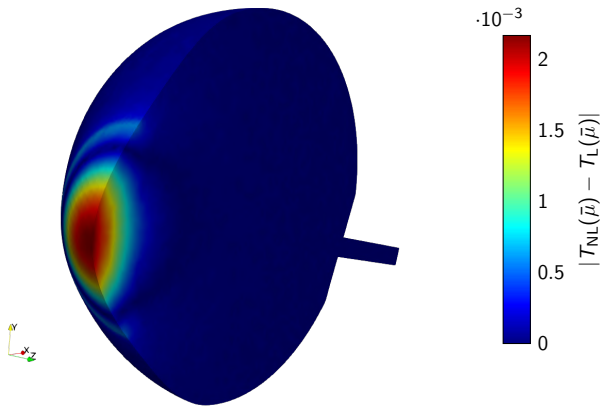


Figure 10: Difference of the temperature between the full model and the linearized model.

Mesh convergence for the high-fidelity model

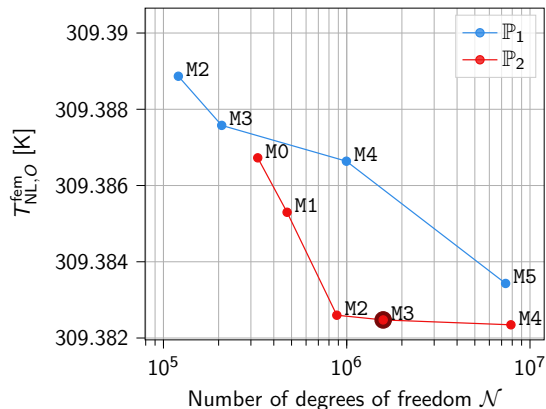
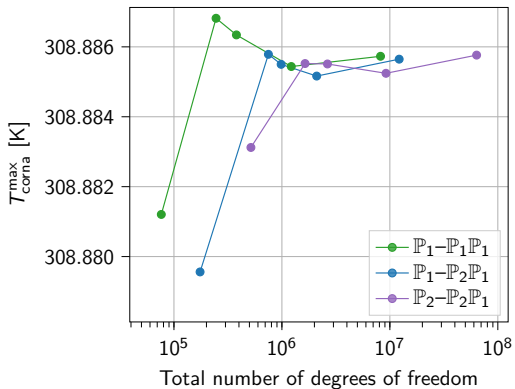
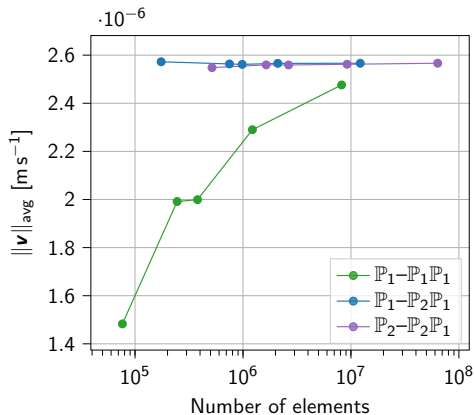


Figure 11: Temperature at the center of the cornea computed with the high-fidelity model $\mathcal{E}_{NL}(\bar{\mu})$, depending on the level of mesh refinement.

Verifications and validations of the coupled heat-fluid model: mesh convergence



(a) Maximal temperature of the cornea.



(b) Mean fluid velocity.

Verifications and validations of the coupled heat-fluid model

Author	T_{amb}	No AH flow	AH flow coupled		
			Prone	Supine	Standing
Scott (2D)	293.15	306.4	–	–	–
Ooi et al. (2D)	298	306.45	–	–	306.9
Karampatzakis et al. (3D)	293	306.81	–	–	307.06
	296	307.33	–	–	307.51
	298	307.69	–	–	307.83
Current model (3D)	293	306.5647	306.56915	306.55899	306.63672
	296	307.09845	307.10175	307.09436	307.14651
	298	307.45746	307.46008	307.45432	307.49222

Verifications and validations of the coupled heat-fluid model

Position	Reference	Maximum velocity [m s ⁻¹]	Average velocity [m s ⁻¹]	Pressure [mmHg]
Supine	Wang et al.	$9.44 \cdot 10^{-4}$	$4.1 \cdot 10^{-5}$	13.50 – 13.58
	Murgoitio-Esandi et al.	$6 \cdot 10^{-5}$	n/a	n/a
	Bhandari et al.	n/a	$9.88 \cdot 10^{-6}$	n/a
	Current model	$2.59 \cdot 10^{-5}$	$3.21 \cdot 10^{-6}$	15.42 – 15.59
Standing	Wang et al.	$9.6 \cdot 10^{-4}$	$2.5 \cdot 10^{-4}$	13.50 – 13.59
	Bhandari et al.	n/a	$5.88 \cdot 10^{-5}$	n/a
	Current model	$2.76 \cdot 10^{-4}$	$5.23 \cdot 10^{-5}$	15.28 – 15.72

Reduced Basis Method

Problem considered

Given $\mu \in D^\mu$, evaluate the output of interest

$$s_N(\mu) = \ell(\mathbf{T}^{\text{rbm},N}(\mu); \mu)$$

where $\mathbf{T}^{\text{rbm},N}(\mu) \in V_N$ is the solution of

$$a(\mathbf{T}^{\text{rbm},N}(\mu), v; \mu) = f(v; \mu) \quad \forall v \in V_N$$

► *Snapshots matrix:*

$$\mathbb{Z}_N = [\xi_1, \dots, \xi_N] \in \mathbb{R}^{\mathcal{N} \times N},$$

Reduced Basis Method

Problem considered

Given $\mu \in D^\mu$, evaluate the output of interest

$$s_N(\mu) = \ell(\mathbf{T}^{\text{rbm},N}(\mu); \mu)$$

where $\mathbf{T}^{\text{rbm},N}(\mu) \in V_N$ is the solution of

$$a(\mathbf{T}^{\text{rbm},N}(\mu), v; \mu) = f(v; \mu) \quad \forall v \in V_N$$

- ▶ *Snapshots matrix:*

$$\mathbb{Z}_N = [\xi_1, \dots, \xi_N] \in \mathbb{R}^{N \times N},$$

- ▶ Projection onto V_N :

$$\underline{\underline{\mathbf{A}}}_N(\mu) := \mathbb{Z}_N^T \mathbf{A}(\mu) \mathbb{Z}_N \in \mathbb{R}^{N \times N} \text{ and}$$

$$\mathbf{f}_N(\mu) := \mathbb{Z}_N^T \mathbf{f}(\mu) \in \mathbb{R}^N,$$

Reduced basis resolution

Input: $\mu \in D^\mu$,

- ▶ Construct $\underline{\underline{\mathbf{A}}}_N(\mu)$, $\mathbf{f}_N(\mu)$ and $\mathbf{L}_{N,k}(\mu)$,
- ▶ Solve $\underline{\underline{\mathbf{A}}}_N(\mu) \mathbf{T}^{\text{rbm},N}(\mu) = \mathbf{f}_N(\mu)$,
- ▶ Compute outputs

$$s_{N,k}(\mu) = \mathbf{L}_{N,k}(\mu)^T \mathbf{T}^{\text{rbm},N}(\mu).$$

Output: Numerical solution $\mathbf{T}^{\text{rbm},N}(\mu)$ and outputs $s_{N,k}(\mu)$.

Affine decomposition^a

- ▶ We want to write $\underline{\underline{\mathbf{A}}}(\mu) = \sum_{q=1}^{Q_a} \beta_A^q(\mu) \underline{\underline{\mathbf{A}}}^q$, and $\mathbf{F}(\mu) = \sum_{q=1}^{Q_f} \beta_F^q(\mu) \mathbf{F}^q$.
- ▶ Compute and store $\underline{\underline{\mathbf{A}}}_N^q = \underbrace{\mathbb{Z}_N^T \underline{\underline{\mathbf{A}}}^q \mathbb{Z}_N}_{\text{independent of } \mu}$ and $\mathbf{F}_N^q = \mathbb{Z}_N^T \mathbf{F}^q$.
- ▶ Hence, $\underline{\underline{\mathbf{A}}}_N(\mu) = \sum_{q=1}^{Q_a} \beta_A^q(\mu) \underline{\underline{\mathbf{A}}}_N^q$ and $\mathbf{F}_N(\mu) = \sum_{q=1}^{Q_f} \beta_F^q(\mu) \mathbf{F}_N^q$.

^aPrud'homme *et al.* *Journal of Fluids Engineering*. (2002)

Affine decomposition^a

- ▶ We want to write $\underline{\underline{\mathbf{A}}}(\mu) = \sum_{q=1}^{Q_a} \beta_A^q(\mu) \underline{\underline{\mathbf{A}}}^q$, and $\mathbf{F}(\mu) = \sum_{q=1}^{Q_f} \beta_F^q(\mu) \mathbf{F}^q$.
- ▶ Compute and store $\underline{\underline{\mathbf{A}}}_N^q = \mathbb{Z}_N^T \underline{\underline{\mathbf{A}}}^q \mathbb{Z}_N$ and $\mathbf{F}_N^q = \mathbb{Z}_N^T \mathbf{F}^q$.
- ▶ $a(T, v; \mu) = \sum_{q=1}^4 \beta_A^q(\mu) a^q(T, v)$ with

$$\beta_A^1(\mu) = k_{\text{lens}} \quad a^1(T, v) = \int_{\Omega_{\text{lens}}} \nabla T \cdot \nabla v \, dx$$

$$\beta_A^2(\mu) = h_{\text{amb}} \quad a^2(T, v) = \int_{\Gamma_{\text{amb}}} T v \, d\sigma$$

$$\beta_A^3(\mu) = h_{\text{bl}} \quad a^3(T, v) = \int_{\Gamma_{\text{body}}} T v \, d\sigma$$

$$\beta_A^4(\mu) = 1 \quad a^4(T, v) = \int_{\Gamma_{\text{amb}}} h_r T v \, d\sigma + \sum_{i \neq \text{lens}} k_i \int_{\Omega_i} \nabla T \cdot \nabla v \, dx$$

^aPrud'homme *et al.* *Journal of Fluids Engineering*. (2002)

Affine decomposition^a

- ▶ We want to write $\underline{\underline{\mathbf{A}}}(\mu) = \sum_{q=1}^{Q_a} \beta_A^q(\mu) \underline{\underline{\mathbf{A}}}^q$, and $\mathbf{F}(\mu) = \sum_{q=1}^{Q_f} \beta_F^q(\mu) \mathbf{F}^q$.
- ▶ Compute and store $\underline{\underline{\mathbf{A}}}_N^q = \mathbb{Z}_N^T \underline{\underline{\mathbf{A}}}^q \mathbb{Z}_N$ and $\mathbf{F}_N^q = \mathbb{Z}_N^T \mathbf{F}^q$.
- ▶ $f(v; \mu) = \sum_{p=1}^2 \beta_F^p(\mu) f^p(v)$

$$\beta_F^1(\mu) = h_{\text{amb}} T_{\text{amb}} + h_r T_{\text{amb}} - E$$

$$\beta_F^2(\mu) = h_{\text{bl}} T_{\text{bl}}$$

$$f^1(v) = \int_{\Gamma_{\text{amb}}} v \, d\sigma$$

$$f^2(v) = \int_{\Gamma_{\text{body}}} v \, d\sigma$$

^aPrud'homme *et al.* *Journal of Fluids Engineering*. (2002)

Offline / Online procedure

Offline:

- ▶ Solve N high-fidelity systems depending on \mathcal{N} to form \mathbb{Z}_N ,
- ▶ Form and store $\mathbf{F}_N^p(\xi_i)$
- ▶ Form and store $\underline{\mathbf{A}}_N^q(\xi_i)$

Online: independant of \mathcal{N}

Given a new parameter $\mu \in D^\mu$,

- ▶ Form $\underline{\mathbf{A}}_N(\mu) : O(Q_a N^2)$,
- ▶ Form $\mathbf{F}_N(\mu) : O(Q_f N)$,
- ▶ Solve $\underline{\mathbf{A}}_N(\mu) \mathbf{T}^{\text{rbm}, N}(\mu) = \mathbf{F}_N(\mu) : O(N^3)$,
- ▶ Compute $s_N(\mu) = \mathbf{L}_N(\mu)^T \mathbf{T}^{\text{rbm}, N}(\mu) : O(N)$.

Error bound^a $\Delta_N(\mu)$

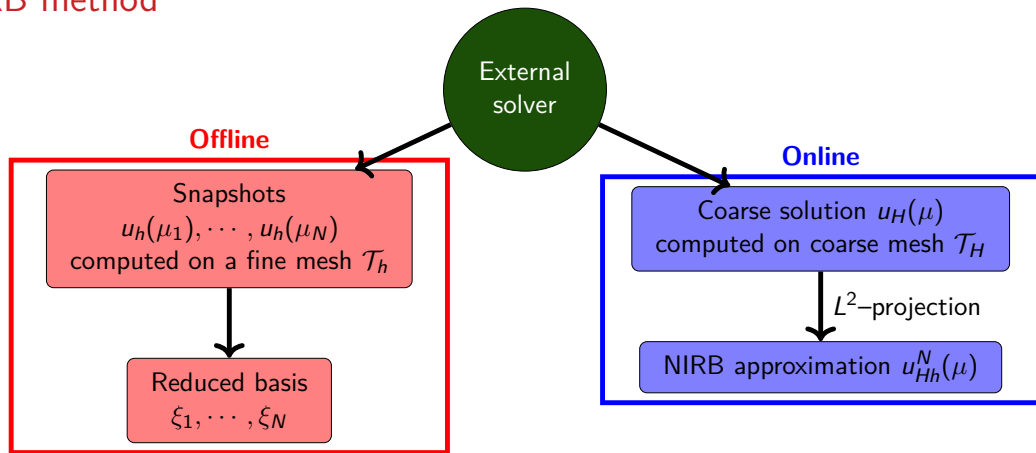
Such an error bound can be constructed efficiently from the *residual* r of the variational problem:

$$r(v, \mu) := \ell(v; \mu) - a(T^{\text{rbm}, N}(\mu), v; \mu) \quad \forall v \in V$$

a lower bound $\alpha_{\text{lb}}(\mu)$ of the coercivity constant $\alpha(\mu)$ of $a(\cdot, \cdot; \mu)$, and the affine decomposition of a and f :

$$\Delta_N^s(\mu) := \frac{\|r(\cdot, \mu)\|_{V'}^2}{\alpha_{\text{lb}}(\mu)}$$

^aPrud'homme *et al.* *Journal of Fluids Engineering*. (2002)

NIRB method^a^aChakir & Maday *Comptes Rendus Mathématique*. (2009)

NIRB method^a

Instead of solving the system $\underline{\underline{\mathbf{A}}}^N(\mu) \mathbf{U}_h^N(\mu) = \mathbf{F}^N(\mu)$ in the online stage and construct the solution by :

$$u_h^N(\mu) = \sum_{i=1}^N \mathbf{U}_{h,i}^N(\mu) \xi_i$$

Let's denote by $\Pi_N u_h$ the L^2 - projection of $\mathbb{F}\mathbb{E}$ approximation u_h in the space X_h^N :

$$\Pi_N u_h(\mu) = \sum_{i=1}^N \alpha_i^{N,h}(\mu) \xi_i$$

Due to the orthonormalization of basis function ξ_i , $\alpha_i^{N,h}(\mu)$ are defined by :

$$\alpha_i^{N,h}(\mu) = \langle u_h(\mu), \xi_i \rangle_{L^2}$$

^aChakir & Maday *Comptes Rendus Mathématique*. (2009)

- ▶ **Coarse** triangulation : $\{\mathcal{T}_H\}_H$ with $H \gg h$,
- ▶ new finite element space : X_H such that $\mathcal{N}_H = \dim(X_H) \ll \dim(X_h) = \mathcal{N}_h$,
- ▶ the computation of $u_H(\mu) \in X_H$ is less expensive than the one of $u_h(\mu) \in X_h$

The **NIRB method** consists in proposing another alternative of $\alpha_i^{N,h}(\mu)$ defined by :

$$\alpha_i^{N,H}(\mu) = \langle u_H(\mu), \xi_i \rangle_{L^2},$$

with $u_H(\mu)$, an approximate solution of the high-fidelity problem in the coarse triangulation.